ELSEVIER

Chemical Engineering Journal 138 (2008) 95–102

Chemical Engineering Journal

www.elsevier.com/locate/cej

# An experimental investigation of scrubber internals at conditions of low pressure

Trond Austrheim[a], Lars H. Gjertsen[a], Alex C. Hoffmann[b,*]

[a] *Statoil ASA, 7005 Trondheim, Norway*

[b] *Department of Physics and Technology, University of Bergen, Allegt. 55, 5007 Bergen, Norway*

Received 20 June 2006; received in revised form 11 May 2007; accepted 22 May 2007

**Abstract**

This paper reports experimental results for the performance of natural gas demisting equipment (natural gas scrubbers), and on basis of this discusses possible improvements in the design of gas scrubbers. The separation efficiency and pressure drop of gas scrubber internals: a vane-type inlet, a mist mat and a cyclone deck, for two gas–liquid systems: air–water and air–Exxsol were determined at a range of gas and liquid flows. To interpret results, a model for the cut size of an axial flow cyclone is given. The results show that when reentrainment limits the separation performance of the scrubber the separation performance varies with the nature of the liquid injected, so that design on basis of an air–water system has to be done with caution. The results and the analysis presented further indicate that the *K*-value, although generally a good evaluation parameter, does not take into account some significant effects, such as the nature of the fluids, changes in the free area for flow, e.g. in the mist mat, and the action of scrubber internals in general. The separation efficiency is shown to be dominated by reentrainment from the cyclone deck at the liquid loadings and gas flows used, loadings and flows which are typical for an industrial scrubber.



*Keywords:* Gas scrubber; Souders–Brown equation; Inlet; Mist mat; Axial flow cyclone; Experiments; Organic liquid

## 1. Introduction

### 1.1. Demisting in natural gas production

The exploration of oil and gas fields is moving towards smaller and more remote fields. To make this feasible more cost effective processing methods must be found. The goal is to perform offshore gas/liquid and liquid/liquid separation sub-sea, as a high-pressure separation process, avoiding expensive topside facilities, facilitating the separation processes themselves, reducing the amount of unwanted products to be transported and making it possible to to reclaim gas at a high pressure, making recompression before pipeline transport unnecessary.

Such a solution, however, requires improved separator design, since expenses related to unsatisfactory separator performance will be much higher. Also, due to higher installation costs, more compact separators will be needed, requiring more rigorous separator design.

* Corresponding author. Tel.: +47 5558 2876; fax: +47 5558 9440.
*E-mail address:* Alex.Hoffmann@ift.uib.no (A.C. Hoffmann).

1385-8947/$ – see front matter © 2007 Elsevier B.V. All rights reserved.
doi:10.1016/j.cej.2007.05.048

Liquid is removed from the gas in all kinds of gas processing facilities for a number of reasons such as:

- prevent breakdown of rotating equipment like expanders, compressors and turbines;
- prevent foaming in gas dryers;
- prevent hydrate formation or other forms of fouling in downstream equipment;
- to keep water or hydrocarbon dew point within sales gas or transport specifications;
- prevent loss of expensive and/or destructive chemicals such as, e.g. glycols or amines;
- protect burners, catalysts, etc.;
- air pollution control.

For the process of separating liquid and gas, two main types of vessel exist—the horizontally oriented and the vertically oriented. The former are mostly used when large amounts of liquid need to be handled, e.g. inlet separators on platforms. The vertical vessels, which are the focus of this article, are used when the fluid has a large gas to liquid ratio. These latter are often referred to as gas scrubbers. Such scrubbers mostly contain different types of separation equipment in series.

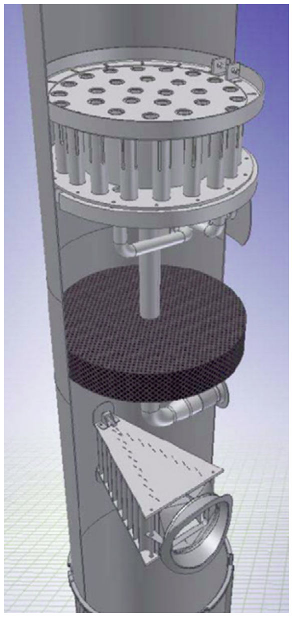

Fig. 1. Diagram of the type of scrubber configuration investigated here. Lowest is the vane inlet, then the mist-mat and on top the cyclone deck, the present cyclone deck contains only seven cyclones.

A sketch of the type of scrubber investigated here is shown in Fig. 1 (note that there are only seven cyclones in the rig used here). The inlet vane distributes the incoming liquid-laden gas over the cross-section, and separates some of the liquid from the gas. The mist-mat may act as a further separator at low gas flows and liquid loading, or as a coalescer for the cyclone deck at high loadings. The deck of axial flow cyclones (AFCs), or once-through cyclones, working in parallel is the last separation step.

Huge costs are associated with mal-functioning scrubbers, mainly due to reduced income because of the resulting operational problems, but modifications and reconditioning of process equipment can also be a significant item of expenditure. Moreover, scrubber efficiency is often a bottleneck in the production, so that efficiency improvements can increase the production capacity [1].

### 1.2. Relevant theory

#### 1.2.1. The Souders–Brown equation

The most used expression for sizing of gas scrubbers is the expression developed by [2] for sizing of fractionating columns. This expression involves an empirically quantified factor known as the Souders–Brown value, the $K$-value, or the Gas Load Factor (GLF). In this publication, the term $K$-value will be used. The basis of the Souders–Brown expression is a force balance resolved in the vertical direction on a spherical droplet in an upward flowing gas in a gravity field. When the droplet is held stationary, i.e. moving at its terminal velocity relative to the gas $u_{\mathrm{g,set}}$, the flow force, $F_\mathrm{r}$ balances the gravity force $G_\mathrm{d}$:

$$F_\mathrm{r} = C_\mathrm{d} A_\mathrm{d} \frac{1}{2} \rho_\mathrm{g} u_{\mathrm{g,set}}^2 = G_\mathrm{d} = \frac{\pi}{6} d_\mathrm{d}^3 g(\rho_\mathrm{l} - \rho_\mathrm{g}),$$

where $C_\mathrm{d}$ is the drag coefficient, $A_\mathrm{d}$ the projected area of the droplet, $\pi d_\mathrm{d}^2/4$ with $d_\mathrm{d}$ the droplet diameter, and $\rho_\mathrm{g}$ and $\rho_\mathrm{l}$ are the densities of the gas and liquid, respectively. This gives:

$$u_{\mathrm{g,set}} \sqrt{\frac{\rho_\mathrm{g}}{\rho_\mathrm{l} - \rho_\mathrm{g}}} = \sqrt{\frac{4 g d_\mathrm{d}}{3 C_\mathrm{d}}}. \tag{1}$$

The right-hand-side of the equation is the definition of the $K$-value:

$$K = \sqrt{\frac{4 g d_\mathrm{d}}{3 C_\mathrm{d}}}. \tag{2}$$

Thus, if $C_\mathrm{d}$ is constant, designing and operating a column at a constant $K$-value means that, irrespective of e.g. the pressure, a droplet of a given diameter will just not be transported upwards and out of the column. In equipment or experiment design the $K$-value is evaluated from the left-hand-side of Eq. (1).

In practice $C_\mathrm{d}$ varies with the droplet Reynolds number, $Re_\mathrm{r} = \rho_\mathrm{g} u_{\mathrm{g,set}} d_\mathrm{d}/\mu$, except for high values of $Re_\mathrm{r}$, where Newton's law states that it is constant and about equal to 0.43. At low $Re_\mathrm{r}$, the well-known relation of Stokes states that:

$$C_\mathrm{d} = \frac{24}{Re_\mathrm{r}},$$

while a general empirical expression due to [3] valid for $Re_\mathrm{r} < 1000$ is:

$$C_\mathrm{d} = \frac{24}{Re_\mathrm{r}} \left(1 + \frac{Re_\mathrm{r}^{2/3}}{6}\right). \tag{3}$$

This is sufficient for most gas scrubbers in practice.

The paper of Souders and Brown thus is focused on terminal settling in a gravity field, and shows that a column has to be designed for a lower gas velocity at higher pressures.

In practice, when designing a column to avoid that the upwards velocity entrains droplets, the recommended $K$-value is $K < 0.1$ m/s for low-pressure applications; often a safety margin of 50% is added for vessels without internals. For increasing pressures the critical $K$-value has been seen to decline. This is not surprising, since increasing pressure in oil/gas applications is often accompanied by a decrease in interfacial tension and thereby a decrease in the droplet sizes. Svrcek and Monnery [4] recommend (for separators with a mesh pad) decreasing the $K$-value with 25% for 85 bar pressure.

Obviously, if a separator is equipped with separation equipment, e.g. a mist-mat or cyclones, it can operate at a higher $K$-value than that required if it simply separates by settling against the flow in an empty separation space. In fact, the $K$-value at which a given separator can operate without entrainment can be seen as a measure of its compactness, and in practice some scrubbers can operate at $K$-values up to 0.3 m/s [5].

### 1.3. Strategy for modelling AFC separation performance

Most cyclone models in the literature are geared to reverse-flow, cylinder-on-cone cyclones with tangential inlets, although a couple have been derived for axial flow cyclones [6,7].

It is also possible to apply the classical cyclone model of Rosin et al. [8,9], which is eminently suitable for axial flow cyclones, to predict the cut size. This model was formulated for tangential-inlet cyclones, and requires the inlet velocity and the dimension of a rectangular inlet.

To give an impression of the cut-size of the cyclones in the present work we report that the adapted model of Rosin et al. predicts cut-sizes of 3.5 and 3.9 μm for water and Exxsol, respectively, with the rig operating at 4 bar pressure with a total volumetric gas flow of 0.183 $m^3/s$. There is thus not much difference between the two liquids, and the cut sizes predicted are far lower than the droplet sizes encountered in the equipment at these pressures.

## 2. Experimental

### 2.1. Rig

The rig is designed for measurements of the removal efficiency of scrubber-internals like inlet arrangements, mist mats, vane-packs and demisting cyclones. The scrubber section is equipped with several windows so that droplet- and flow-phenomena can be studied. As liquids, water and Exxsol D60 were used. Exxsol D60 is a dearomatized aliphatic hydrocarbon, where the major components are normal paraffin's, isoparaffin's and cycloparaffin's. The liquid contains very low levels of hazardous air pollutants, and has a low vapour-pressure, making it suitable for indoor use. More information about the fluids used is given in Table 1.

In Fig. 2, a sketch of the most important features of the rig is given. The gas enters the rig through an 80 mm pipe and is distributed over the cross-section of the 0.39 m i.d. scrubber cross-section by inlet vanes. The air is supplied from two compressors that deliver a constant mass-rate of 0.88 kg/s at approximately 7 bar. The pressure in the scrubber, and, hence, the volumetric gas-flow, is controlled by a manually operated throttle valve in the piping upstream the scrubber inlet. This means that the volumetric flow and gas density cannot be controlled independently. The liquid is fed through a nozzle in either the upstream piping or in the vessel itself (optional).

Liquid that is separated in the inlet arrangement or other internals without internal drain pipes is collected in the bottom of the vessel and is fed back to the liquid reservoir. The liquid collected in the demisting equipment equipped with an internal drain system, is collected on a scale below the vessel while the liquid carry-over from the scrubber is separated in a large-capacity filter-coalescer and then collected on a separate scale. These two scales make it possible to calculate the liquid mass-balance, and have drains connected to the liquid reservoir to empty the scale-vessels when they are filled. All the monitored parameters from the rig, such as flow rates, pressures, differential pressures, temperatures and accumulated liquid on the scales, are logged on a PC that monitors and controls parts of the rig. The system logs all parameters with an interval of two seconds, and when logging is finished, the average of all parameters are automatically written to a file and stored on the hard drive.

Table 1
Physical properties of fluids at 20 °C and 1 bar

| | Density [kg/m$^3$] | Viscosity [cP] | Air/liquid interfacial tension [mN/m] |
|---|---|---|---|
| Air | 1.19 | 0.0184 | |
| Exxsol D60 | 790 | 1.40 | 24.3 |
| Water | 1000 | 0.89 | 72.8 |

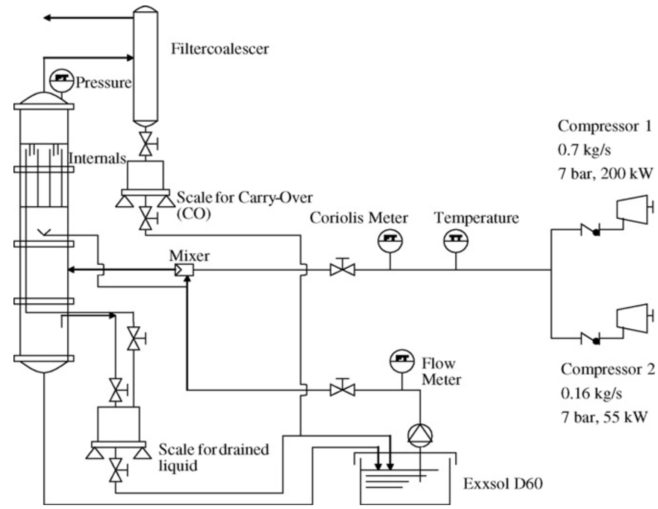


Fig. 2. A sketch of the experimental rig used.

Two geometrical configurations have been used, shown in Fig. 3. The configuration to the left was used in order to check the performance of the cyclones in combination with an inlet vane arrangement upstream. Liquid was introduced either through a liquid nozzle above the inlet vanes or through a nozzle in the upstream piping. The configuration to the right in the figure is the standard setup.

Since varying amounts of liquid needed to be injected in the scrubber, different nozzles were used in different tests. The nozzles were produced by Delavan Spray Technologies and are of types BLM-5, BF-12 and BNM-39. Two of the nozzles (BLM-5 and BF-12) produces a spray angle of 90° while the last produces

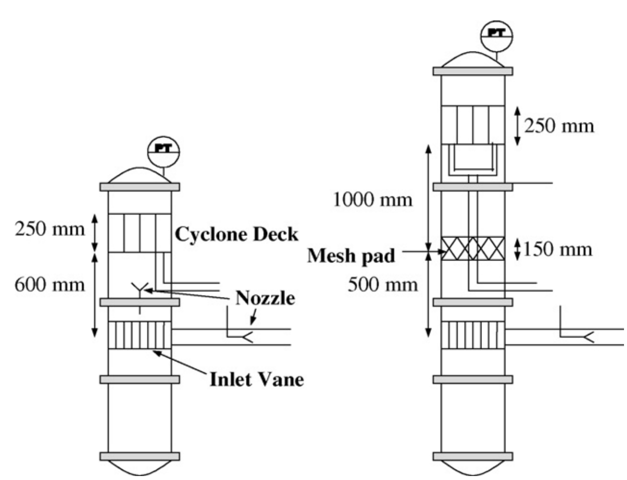


Fig. 3. The two different test setups.

Fig. 4. The inlet internal.

a spray angle of 90–120°, dependent on the pressure (a larger pressure gives smaller angle for this design).

### 2.2. Internals

The *inlet* was, as mentioned of the vane type, where the incoming gas exits through a series of vanes at the sides to be well distributed over the column cross-section (see Fig. 4). The top and bottom plates were transparent to give a view of the vanes themselves. The length of the inlet internal was 0.39 m, it was charged from a 0.08 m i.d. pipe, and it covered 0.0474 $m^2$, or 39.6% of the column's horizontal cross-section.

The *mesh pads* used have been produced by Costacurta S.p.A Vico, and are identical to the mesh pad 'Style A' investigated experimentally and theoretically by Brunazzi and Paglianti [10]. The mesh pad was constructed in stainless steel, AISI 304 and the general properties of a the mat were: wire diameter: 0.27 mm; packing density 144 kg/$m^3$; specific area: 274 $m^2/m^3$; void fraction: 0.95; pad thickness, 0.15 m and equivalent mesh diameter 2.35 mm.

Several sketches of *axial flow cyclone* (AFC) geometries are given in open literature [11–17]. Only the works of [13] and [16] contain sufficient details to reproduce the cyclones and since the work by Ng was not published at the start of this project, the Verlaan cyclone was chosen as the AFC in the standard setup for the scrubber. A sketch of the Verlaan cyclone configuration used, including the vortex finder that was installed at a later stage (see below) is shown in Fig. 5.

The exit angle from the vane blades was 45dgr, and the vertically oriented slits are designed with a sharp inner edge to aid the liquid separation.

One common principle of commercial AFC's is not included in the Verlaan cyclone, namely the use of a secondary gas flow to help the liquid through the drainage slits. There are two ways of adding the secondary flow; either by recycling some gas back to the low-pressure zone downstream of the swirl generator in the centre of the cyclone body, or by adding secondary outlets at the top of the drain chamber.

The cyclones have been arranged in parallel in a cyclone deck as shown in Fig. 1. The packing density of such a deck can be

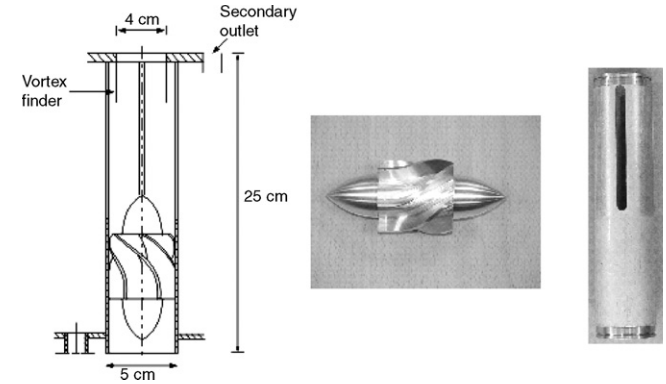


Fig. 5. The swirl tube used, designed on basis of Verlaans [13] swirl tube, except for the vortex finder and the secondary outlet, which were installed later (see below). Photographs of the swirl element and the tube section are also shown.

defined as the ratio of the sum of the cyclone cross sections to the total scrubber cross section. The packing density in this cyclone deck was 0.115. There were seven cyclones in the deck.

## 3. Results and discussion

We first report the results obtained for the cyclone deck, and then for the inlet and the mistmat.

### 3.1. Cyclone deck

In this section, liquid flows are mostly reported as volume% of the gas flow. These values cannot be taken as precise liquid loadings in the flow entering the cyclones because the liquid distribution was not uniform over the cross-section, causing the liquid loading to the individual cyclones to be non-uniform. This was caused by flow from the inlet creating a swirling motion in the gas between the inlet and the cyclones, which was assymmetical with respect to the scrubber axis. The experiments were carried out under the same conditions and with the same equipment, and trends are therefore reliable. We will give an estimate of experimental error below.

Fig. 6 shows results obtained in this work using an air–water system, together with results obtained by [13], who also used air and water.

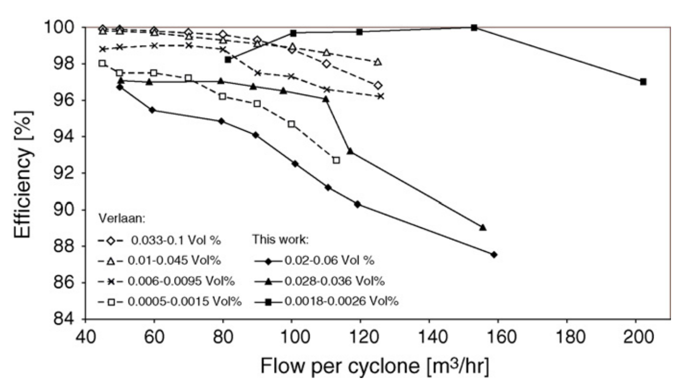


Fig. 6. A collocation of the results obtained by Verlaan and results obtained in this work. [13] tested one cyclone with a gas density of 7.5 kg/$m^3$, while in this work seven cyclones working in parallel at gas densities ranging from 2.1 to 7.5 kg/$m^3$ were tested.

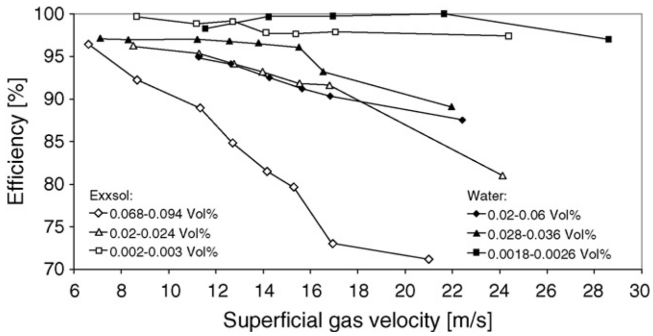


Fig. 7. A comparison between the cyclone efficiency with Exxsol D60 and with water. Water is easier to separate than Exxsol D60 for all tested cases.

The figure clearly shows that in all cases, except for one, the separation efficiency drops off as the gas flow increases. All cyclone models, including the model for AFCs presented above, show that if the droplets are so small that the cyclone separation efficiency is determined by the droplet size, one would expect an increase in efficiency with increasing volumetric gas flow. It is also well known that an increasing loading, at least in cyclonic dedusters with tangential inlets also leads to an increase in the separation efficiency [15].

However, if re-entrainment of liquid from the cyclones is the determining factor, the efficiency would intuitively be expected to drop off with higher volumetric gas flow and liquid loadings.

At these low pressures and large liquid flow rates, the liquid is likely to exist in the form of quite large droplets, larger than the cyclone cut size, and the droplet size should not play an important role – if any at all – in determining the separation efficiency. The atypical behaviour of the curve corresponding to the lowest loading, where efficiency increases with increasing gas flow rate, is consistent with the notion that in this case a sufficient amount of liquid was dispersed into small droplets comparable to the cut-size of the cyclone, so that its efficiency was limited by its capture of small droplets [15].

The model derived above, as mentioned, predicts cut-sizes for the cyclones of about 4 μm, which is probably well below the droplet size dominating in the flow under these conditions.

The physical properties of water, high interfacial tension, relatively low viscosity and high density, makes it easier to separate than hydrocarbons. Since the main focus for this work is to investigate scrubbers for hydrocarbon services, the test fluid for the rest of the experiments reported here is Exxsol D60. In particular, the same tests in identical geometries to those shown in Fig. 6 have also been carried out with Exxsol as liquid. The results are compared in Fig. 7. As opposed to the comparison in Fig. 6, the results are here compared in terms of the superficial velocity in the cyclones, $v_{sg}$.

The separation efficiency of the cyclones is much lower when Exxsol is used as liquid instead of water. In fact, the absolute liquid carry-over is up to three times as large when Exxsol is used. This clearly underlines the importance of taking into account the fluid properties when lab-results are used as basis for the design of real scrubbers. The relatively minor difference in cut sizes using the two liquids, predicted by the model above, cannot explain such a large difference in separation performance.

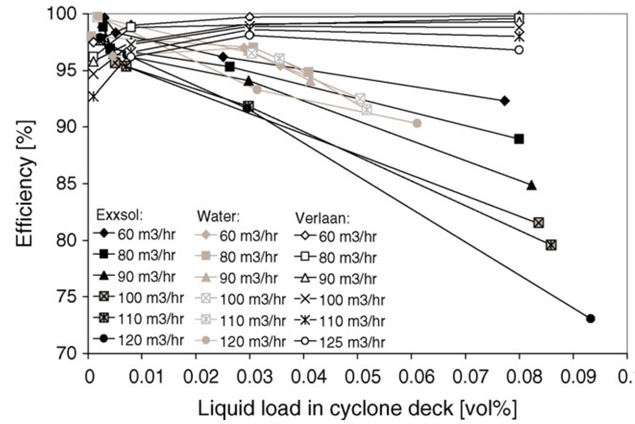


Fig. 8. The efficiency of the cyclones in this work shows a different liquid load dependence to the cyclone tested by Verlaan.

The results from Figs. 6 and 7 have been plotted against liquid load to the cyclone deck in Fig. 8. This plot shows that in this work the efficiency drops with an increase in liquid load for both water and Exxsol, while Verlaan reported an increased efficiency with increasing liquid load.

A number of features are, or may have been, different between this rig and that of Verlaan to explain this difference in the results. Three design features, which may differ, but for which there is insufficient information in the work of Verlaan, are:

(a) For manufacturing reasons, the drainage slits did not extend right to the top of the tubular section, leaving about 1 cm above the slits where liquid could build up and be reentrained, possibly overwhelming the edge at the top of the tube section designed to avoid reentrainment.
(b) The tube walls were relatively thick in this rig, and the angle of the slits therefore not very steep.
(c) The design of the swirl vanes in the present rig may have been different, explaining perhaps the superior performance at low liquid loadings (<0.01 vol.%).

Also three operational features may cause differences in the performance:

(d) The size of droplets generated in the present experiments may be different, and
(e) An uneven liquid and/or gas distribution between the parallel cyclones in the present rig may also cause a difference in performance.
(f) As mentioned the gas mass rate from the compressors was constant, and the volumetric flow controlled by varying the pressure in the rig, while the experiments of Verlaan were carried out at a constant pressure, equal almost to the highest pressure used here.

Of these, only items (a), (b) and (e) can potentially cause a difference in the trend in efficiency with liquid load.

To improve the performance, two modifications were made, as mentioned before and indicated in Fig. 5: a vortex finder was installed to ameliorate problems with reentrainment from the top of the cyclones, and a secondary outlet to help with the transport of liquid through the drainage slits.

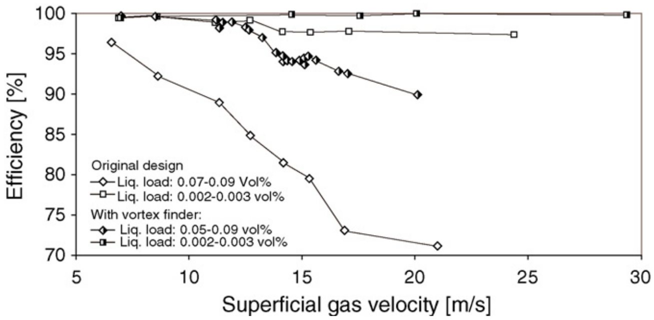


Fig. 9. Efficiencies with and without vortex finder.

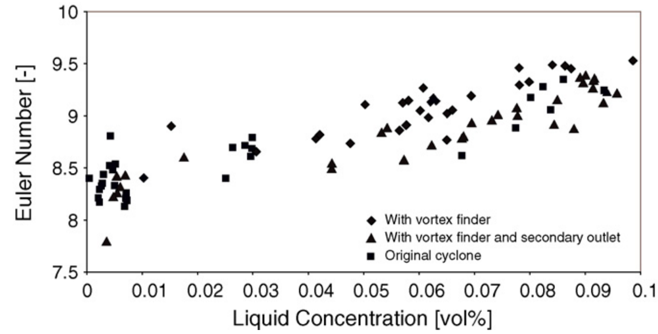


Fig. 10. Pressure drop coefficients in the cyclones for the air/Exxsol experiments.

The installation of the vortex finder improved the cyclone efficiency as can be seen in Fig. 9. At the lowest liquid loadings, the efficiency is close to, or actually at 100%, meaning that it was not possible to detect any liquid in the gas outlet. For the tests with the largest liquid loading and the highest gas flow, the efficiency was improved from 71 to 90%, which is a large improvement for such equipment.

According to all cyclone models, including the AFC model presented above, the installation of a vortex finder should only restrict the length of the separation space, and therefore reduce separation efficiency. This large improvement in efficiency strongly indicates that cyclone efficiency in this work is related to some kind of liquid reentrainment from the cyclone.

The secondary outlet did not improve performance, and the results are not reported here. Note that, contrary to other design solutions for secondary flow [11,13,16], the secondary flow in this case could by-pass the cyclones, and thus entrain droplets.

The experimental error in these experiments can be assessed by estimating the error of each measurement, and using Gauss' formula for error propagation. This only yields an estimate of error of less than 0.01%. However, the errors from variations in the process conditions are larger than that. Repeating experiments with a liquid load of 0.1 vol% with the vortex finder installed, distributing the repeat tests among the other tests in a random manner, resulted in an estimate for the standard deviation due to experimental error of 0.25%.

In a number of tests the sensitivity of the results to the position of the liquid injection nozzle was assessed. Some differences in absolute separation efficiencies were found (up to about 2%), but the trends in the data were the same, irrespective of the nozzle position.

The pressure drop over the cyclones and mesh pad was measured in all experiments, except those in the air/water, where the measurements were corrupted due to water in one of the legs in the pressure difference meter.

The results are shown in Fig. 10 in terms of the pressure drop coefficient or Euler number:

$$Eu = \frac{\Delta P}{(1/2)\rho_g v_g^2}$$

The Euler number, *Eu* is a characteristic for the pressure drop over a dry cyclone. When liquid is present, *Eu* becomes dependent on the liquid load. The pressure drop in a reverse flow cyclone with tangential inlet is expected to decrease when liquid (or solid) is introduced [15]. However, the pressure drop in a swirl tube with heavily laden upward flow is expected to increase; a discussion of this issue is given by [16,17]. This is also what is seen in Fig. 10. Although the effects are only slight, the presence of the vortex finder increases the pressure drop, while opening the secondary outlet decreases the pressure drop. The latter result is also consistent with the results of Ng et al.

### 3.2. Inlet vane and mistmat

The setup to the right in Fig. 3 was used for the experiments in this section, seven $K$-values in the range 0.1–0.16 m/s were tested, each at five liquid concentrations.

In this and the following sections, the $K$-value is calculated from the left-hand-side of Eq. (1):

$$K = u_g\sqrt{\frac{\rho_g}{\rho_l - \rho_g}},$$

where $u_g$ is the relevant velocity, in this case the mean axial velocity in the scrubber.

In addition to this, the rig was tuned to find the flooding point of the mesh pad for each liquid concentration by visual observation. The flooding point was defined as the point where the liquid accumulation in the mesh pad reached the top surface, although this is difficult to determine precisely since the transition from a demisting mat to a flooded mat is a gradual one.

The rig design did not allow determination of the individual separation efficiencies of the inlet vane and the mesh pad, but the combined separation efficiency of both scrubber internals can be calculated on basis of the injected liquid and the collected liquid in the cyclones and the filter coalescer.

The known uncertainties in the measurements, and Gauss' formula for error propagation indicated an experimental error of <0.3% in the separation efficiency. In practice, taking into account variabilities in the operating conditions, this uncertainty is likely to have been somewhat higher.

It is customary to design this type of equipment using the $K$-value introduced in Section 1.2.1. The combined efficiency of the inlet vane and the mesh pad is shown in Fig. 11. The flooding point for each curve is also indicated.

It is clear that the flooding point is not just dependent on the $K$-value but also on the liquid concentration. Such a dependency has also been identified by [12]. The reason for this is that liquid

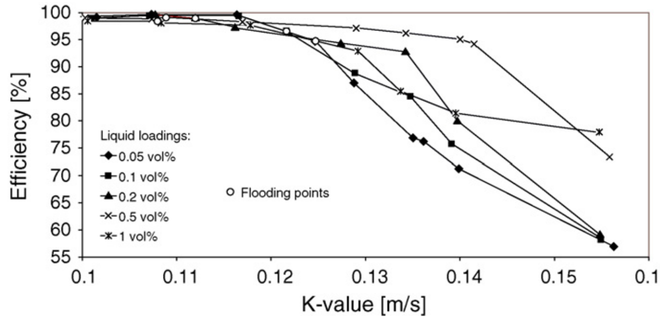


Fig. 11. The efficiency of the inlet vane and mesh pad (the "primary separation efficiency") as function of the gas flow, expressed as the $K$-value.

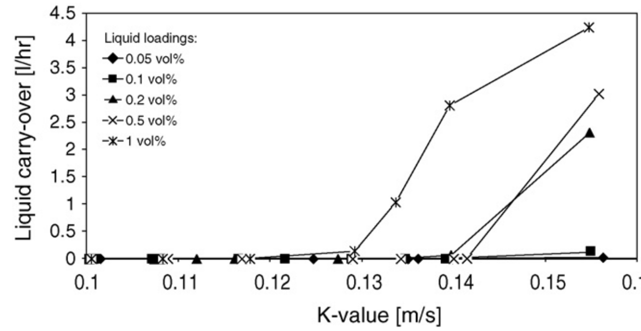


Fig. 13. The absolute liquid carry-over for the experiments where liquid is injected in the upstream piping, and enters the cyclone deck via the mesh pad.

hold-up in or below the mesh pad reduces the free area so that the local gas velocity vectors increases, an effect not accounted for in the K-factor, which, as mentioned, is based on the superficial velocity.

The efficiency never exceeds 99% for the lowest $K$-values where the mesh pad is operated below flooding conditions. One must therefore assume that approximately 1% of the liquid from the inlet vane distributes as fine droplets that are too small to be caught in the mesh and/or that some liquid reentrainment takes place also from the non-flooded mesh. The mesh typically separates all droplets above 15 μm [10].

The fractional efficiency increases with increasing liquid concentration up to 0.5 vol%. However, the absolute liquid carry-over increases with increasing liquid concentration. When the data in Fig. 11 are re-plotted as absolute liquid carry-over from the mest pad, it is clear that the carry-over increases with increasing liquid load and with increasing gas flow.

### 3.3. Total scrubber efficiency

In Fig. 12, a comparison is made of the cyclone efficiency when liquid is introduced through nozzle BN39 on the one hand and when the liquid is entrained from mesh pad on the other.

A superficial gas velocity of 13 m/s corresponds to a $K$-value in the vessel of 0.117 m/s, meaning that the mesh pad is slightly below or slightly above the flooding point, depending on the liquid load. When the mesh pad is below the flooding point, it acts as a conventional separator, and only small droplets below its cut-size pass to enter the cyclones. This explains the reduced efficiency for these points. When the mesh pad is operated above the flooding point, it acts as a coalescer, and larger droplets are entrained to the cyclone deck. At moderate gas flows and liquid loads this liquid is evenly distributed over the cyclones. This applies to the the points marked as '13 m/s, mesh pad' in Fig. 12, and these data agree well with the results obtained by use of nozzle BN39 at the same gas velocity.

However, when the gas flow and liquid load are increased further the liquid above the mesh pad starts to pulsate, and periodically liquid-laden jets will form from the mesh pad. An individual cyclone therefore experiences sudden bursts in liquid load influencing the performance negatively. When the superficial velocity in the cyclones is 23 m/s, the vessel $K$-value is 0.156 m/s. Under these conditions, the efficiencies with the mesh pad is lower than the corresponding ones with the nozzle. This is despite the fact that the mesh pad is placed quite far below the cyclone deck, approximately 0.8 m—a relative large distance in a scrubber.

If the above pulsation and jetting occurs, this influences also the total scrubber efficiency negatively. The absolute liquid carry-over from the scrubber for the experiments reported in Fig. 11 are shown in Fig. 13. The carry-over increases with increasing gas flow ($K$-value) and liquid load.

The over-all efficiency is shown in Fig. 14. As can be seen, the efficiency is above 90% for all experiments. The efficiency decreases with increasing gas and liquid load.

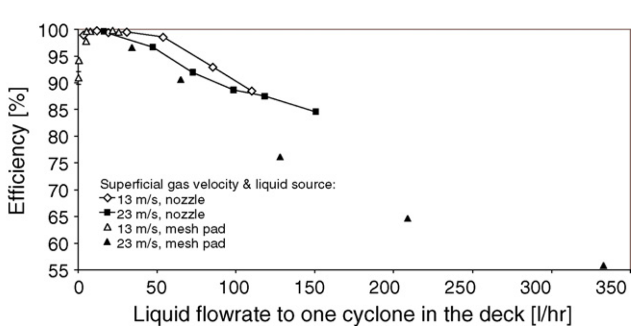


Fig. 12. The cyclone efficiency as function of liquid load when liquid is introduced through nozzle BN39 or as entrainment from the mesh pad.

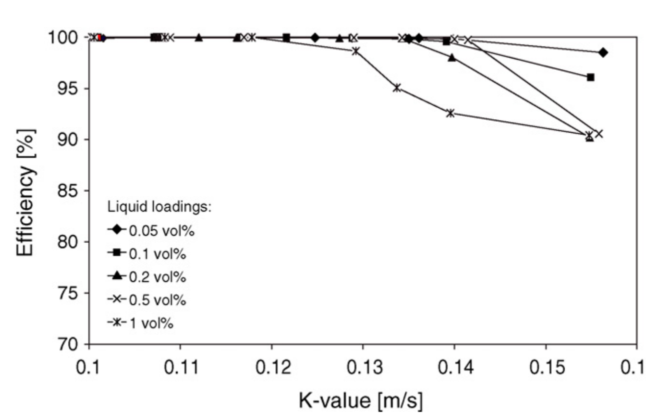


Fig. 14. The total scrubber efficiency of the experiments where liquid is injected in the upstream piping.

## 4. Further discussion and concluding remarks

This work has shown that the $K$-value in general is a good evaluation parameter for scrubbers, even when they are equipped with inlet vanes and mesh pads, although in principle the $K$-value does, as discussed, not describe the separation in such internals correctly. The curves in Figs. 11 and 14 break at approximately the same value for $K$, although corresponding to very different operational conditions.

Nevertheless, also short-comings have been exposed: the $K$-value does in principle not correlate the efficiency of separation internal based on impaction at all. Also the flooding points for the mesh pad were not well correlated by the $K$-value (Fig. 11).

More seriously: the nature of the liquid (Exxsol or water) had a substantial impact on the separation efficiency as seen in Fig. 7. This is probably due to differences in the liquid physical properties, which will influence both the size of liquid droplets in the equipment, and the extent of liquid reentrainment, something that is not described by the $K$-value at all.

In fact, the results indicate that the criterion of $K \leq 0.15$ m/s normally handled for a scrubber to operate with a separation efficiency of more than 99%, which to a large extent is based on experimental results obtained using air–water model systems, may not be sufficient even at low pressure when hydrocarbon liquids are used.

All of the results, and in particular Fig. 9 indicate that the separation efficiency was determined by reentrainment from the cyclone deck. In subsequent publications, we will consider the issue of reentrainment in more detail.

For those cases (mainly for the inlet vane/mistmat combination at low loading) where separation efficiency was limited by fine droplets passing through the internals, further analysis would require knowledge of the in- and outgoing droplet size distributions. An important aim of this work was to investigate how the change of test fluids in an otherwise identical geometry would affect the separation efficiency. Therefore, the present experimental procedure does not give direct control of the droplet size from the nozzles, which will vary with the physical properties of the liquid being atomized. The droplet size will also vary from nozzle to nozzle and with the liquid flow through the nozzles, which is regulated by adjusting the nozzle injection pressure. These variations will, however, at least qualitatively, be consistent with the variations of the average droplet size in an actual industrial installation. In future work it is a priority to measure the droplet sizes in the equipment.

## Acknowledgment

Financial support from the Research Council of Norway through the HiPGaS programme, and the industrial sponsors Statoil AS, ConocoPhillips, Norsk Hydro AS, Vetco, FMC Kongsberg Subsea and Aker-Kværner is highly appreciated.

## References

[1] S.O. Bjørnestad, J. Ophaug, T. Austrheim, K. Vedvik, Resolving operating problems at troll gas plant have also lead to a 40% capacity increase, in: GPA Annual Conference, Barcelona, 2000.

[2] M. Souders, G.G. Brown, Design of fractionating columns. i. entrainment and capacity, Ind. Eng. Chem. 2 (1934) 98–103.

[3] A. Putnam, Integratable form of droplet drag coefficient, ARS J. 10 (1961) 1467–1468.

[4] W.Y. Svrcek, W.D. Monnery, Design 2-phase separators within the right limits, Chem. Eng. Progr. 89 (1993) 53–60.

[5] L.H. Gjertsen, T.V. Løkken, N.M. Marheim, J. Ophaug, Separation efficiency of the troll kollsnes separators and the improvement in their performance, in: GPA 82nd Annual Convention Presentations, New Orleans, 2003.

[6] J.I.T. Stenhouse, M. Trow, The behaviour of uniflow cyclones, in: The Second World Filtration Congress, London, 1979, pp. 151–155.

[7] G. Ramachandran, P.C. Raynor, D. Leith, Collection efficiency and pressure-drop for a rotary-flow cyclone, Filtrat. Sep. 31 (1994) 631–636.

[8] P. Rosin, E. Rammler, W. Intelmann, Principles and limits of cyclone dust removal, Zeit. Ver. Deutscher Ing. 76 (1932) 433–437.

[9] F.A. Zenz, Cyclone design, in: W.-C. Yang (Ed.), Fluidization, Solids Handling, and Processing: Industrial Applications, Noyes Publns, Westwood, NJ, 1999.

[10] E. Brunazzi, A. Paglianti, Design of wire mesh mist eliminators, AIChE J. 44 (1998) 505–512.

[11] R.A. Swanborn, A new approach to the design of gas–liquid separators for the oil industry, Ph.D. thesis, Delft University of Technology, 1988.

[12] A. Bürkholz, Droplet separation, VCH Publishers, 1989, ISBN 0-89573-879-1.

[13] C.C.J. Verlaan, Performance of novel mist eliminators, Ph.D. thesis, Delft University of Technology, 1991, ISBN 90-370-0054-1.

[14] F.T.M. Nieuwstadt, M.A. Dirkzwager, fluid mechanics model for an axial cyclone separator, Ind. Eng. Chem. Res. 34 (1995) 3399–3404.

[15] A.C. Hoffmann, L.E. Stein, Gas Cyclones and Swirl Tubes—Principles, Design and Operation, Springer-Verlag, 2002, ISBN 3-540-43326-0.

[16] S.Y. Ng, Gas–liquid separation using axial flow cyclones, Ph.D. thesis, University of Sheffield, 2005.

[17] S.Y. Ng, G.H. Priestman, R.W.K. Allen, Investigation of flooding, re-entraiment and grade efficiency in axial flow cyclones, Chem. Eng. Res. Des. 84 (2006) 884–894.